Developmental Biology 371 (2012) 235–245

Contents lists available at SciVerse ScienceDirect

Developmental Biology

journal homepage: www.elsevier.com/locate/developmentalbiology

Signaling by FGF4 and FGF8 is required for axial elongation of the mouse embryo

Anne M. Boulet, Mario R. Capecchi *

Howard Hughes Medical Institute, Department of Human Genetics, University of Utah School of Medicine, Salt Lake City, UT 84112, USA

ARTICLE INFO

Article history:
Received 16 July 2012
Received in revised form
16 August 2012
Accepted 21 August 2012
Available online 30 August 2012

Keywords:
Mouse
Embryo
Mesoderm
FGF
Elongation

ABSTRACT

Fibroblast growth factor (FGF) signaling has been shown to play critical roles in vertebrate segmentation and elongation of the embryonic axis. Neither the exact roles of FGF signaling, nor the identity of the FGF ligands involved in these processes, has been conclusively determined. *Fgf8* is required for cell migration away from the primitive streak when gastrulation initiates, but previous studies have shown that drastically reducing the level of FGF8 later in gastrulation has no apparent effect on somitogenesis or elongation of the embryo. In this study, we demonstrate that loss of both *Fgf8* and *Fgf4* expression during late gastrulation resulted in a dramatic skeletal phenotype. Thoracic vertebrae and ribs had abnormal morphology, lumbar and sacral vertebrae were malformed or completely absent, and no tail vertebrae were present. The expression of *Wnt3a* in the tail and the amount of nascent mesoderm expressing *Brachyury* were both severely reduced. Expression of genes in the NOTCH signaling pathway involved in segmentation was significantly affected, and somite formation ceased after the production of about 15–20 somites. Defects seen in the mutants appear to result from a failure to produce sufficient paraxial mesoderm, rather than a failure of mesoderm precursors to migrate away from the primitive streak. Although the epiblast prematurely decreases in size, we did not detect evidence of a change in the proliferation rate of cells in the tail region or excessive apoptosis of epiblast or mesoderm cells. We propose that FGF4 and FGF8 are required to maintain a population of progenitor cells in the epiblast that generates mesoderm and contributes to the stem cell population that is incorporated in the tailbud and required for axial elongation of the mouse embryo after gastrulation.

Introduction

During gastrulation, epiblast cells are recruited to the primitive streak, undergo an epithelial to mesenchyme transition, and ingress through the streak to establish the mesodermal and endodermal germ layers of the embryo. Elongation of the body axis continues from the tail bud after closure of the posterior neuropore. The existence of long term progenitors in the E8.5 mouse primitive streak is strongly suggested by the results of DiI lineage tracing: While most labeled cells exit from the primitive streak, some are maintained in the tailbud for upto 48 h (Wilson and Beddington, 1996). Subsequent analyses have provided experimental evidence that multipotent stem cells contribute to the production of neural tube, notochord and somites in the chick and the mouse (reviewed in (Wilson et al., 2009)). Further studies in the mouse suggest that self-renewing stem cell populations exist in the primitive streak region during gastrulation and in the chordoneural hinge (CNH) after tail bud formation at about the 30 somite stage (Cambray and Wilson, 2002, 2007; Tzouanacou et al., 2009).

The clock and wavefront model has been proposed as a mechanism to explain the orderly formation of somites from the presomitic mesoderm (PSM) (reviewed in (Pourquie, 2001)). The correct timing of segment formation requires oscillations of NOTCH pathway activity, which comprise the segmentation clock, while the wavefront maintains PSM cells in an undifferentiated state. The wavefront appears to be established by opposition of the posterior activity of WNT and FGF/MAPK pathways and rostral retinoic acid pathway activity (Aulehla et al., 2003; Diez del Corral and Storey, 2004; Dubrulle et al., 2001; Dubrulle and Pourquie, 2004; Sawada et al., 2001). Adding another layer of complexity, the clock and wavefront elements are not independent of one another. Some components of the FGF and WNT/β-catenin pathways show oscillating expression (Aulehla et al., 2003; Dequeant et al., 2006; Niwa et al., 2007), and mutations in these pathways affect oscillating expression of the NOTCH pathway components (Aulehla et al., 2003; Dunty et al., 2008; Niwa et al., 2007; Wahl et al., 2007). Mutations in the FGF pathway also

* Correspondence to: Howard Hughes Medical Institute, University of Utah, 15 North 2030 East, Suite 5400, Salt Lake City, UT 84112-5331, USA.
Fax: +1 801 585 3425.
E-mail addresses: anne@genetics.utah.edu (A.M. Boulet), mario.capecchi@genetics.utah.edu (M.R. Capecchi).

0012-1606/$ - see front matter © 2012 Elsevier Inc. All rights reserved.
http://dx.doi.org/10.1016/j.ydbio.2012.08.017

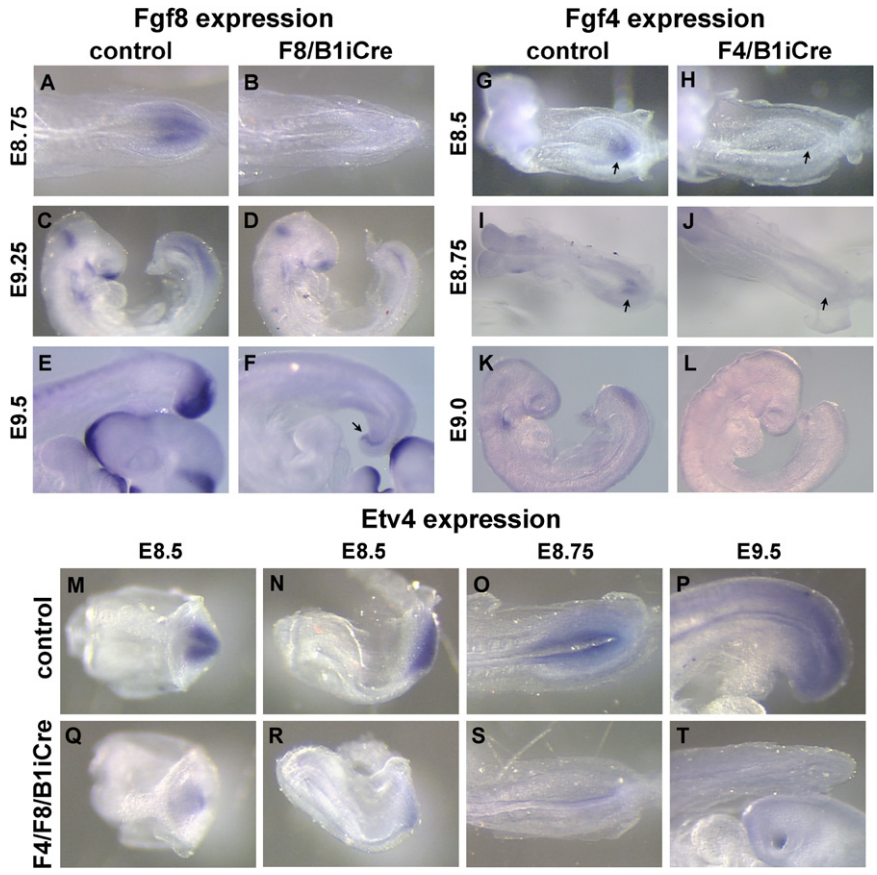

Fig. 1. Loss of *Fgf4* and *Fgf8* expression after recombination mediated by *B1iCre* results in a reduction in FGF signaling in the posterior embryo. (A–F) Whole mount in situ hybridization with an *Fgf8* probe to E8.75 control (A) and *F8*/*B1iCre* mutant (B), E9.25 control (C) and *F8*/*B1iCre* mutant (D), and E9.5 control (E) and *F8*/*B1iCre* mutant (F) embryos. Arrow in (F) points to hindgut. (G–L) *Fgf4* expression in E8.5 control (G) and *F4*/*B1iCre* mutant (H), E8.75 control (I) and *F4*/*B1iCre* mutant (J), and E9 control (K) and *F4*/*B1iCre* mutant (L) embryos. Arrows in (G), (H), (I) and (J) point to the site of *Fgf4* expression in the primitive streak. (M–T) *Etv4* expression, detected by whole mount in situ hybridization, in control embryos at E8.5 (M and N), E8.75 (O), and E9.5 (P), and *F4*/*F8*/*B1iCre* mutant embryos at E8.5 (Q and R), E8.75 (S), and E9.5 (T). (M) and (Q) are ventral views of the primitive streak region; (O) and (S) are dorsal views; and (N), (P), (R) and (T) are lateral views.

affect oscillations of WNT/β-catenin pathway components (Wahl et al., 2007). These observations suggest complex interactions among all three pathways involved in segmentation.

Several lines of evidence indicate that FGF signaling is required for proper segmentation of the mouse embryonic axis. Although *Fgf receptor 1* (*Fgfr1*) null mutants fail to produce mesoderm because primitive streak cells are unable make the epithelial to mesenchymal transition (EMT), hypomorphic or isoform-specific mutants of *Fgfr1* show defects in development of the posterior mesoderm (Partanen et al., 1998; Xu et al., 1999). Extensive analysis in chick and mouse has suggested that *Fgf8* plays a critical role in positioning the formation of somites from the PSM (Dubrulle et al., 2001). A posterior to anterior gradient of FGF protein results from *Fgf8* transcription at the posterior end of the embryo and subsequent degradation of the mRNA as the axis extends. The clock and wavefront model proposes that a specific level of FGF8 maintains PSM cells in an undifferentiated state. When cells are released from the influence of FGF8 as the axis extends, they form the next somite according to the timing established by the segmentation clock. The role of FGF8 cannot be tested directly in *Fgf8* null mutants as they are unable to complete gastrulation (Sun et al., 1999). However, when *Fgf8* expression was eliminated in the mesoderm of early embryos (E7.5-8), no defect in the formation of posterior somites was detectable (Perantoni et al., 2005).

In addition to a proposed role in somite segmentation, FGF signaling also clearly plays a role in axis elongation. Whereas *Fgfr1* null mutants fail to form mesoderm, posterior skeletal truncations are seen in *Fgfr1* hypomorphs (Partanen et al., 1998). Posterior truncation is also observed in embryos lacking FGFR1α isoforms, and these defects were attributed to defective migration of axial mesoderm (notochord) progenitors (Xu et al., 1999). Truncations in the sacral and tail regions of the vertebral column were reported for a conditional knockout of *Fgfr1* in the PSM (Wahl et al., 2007). Finally, severe axis truncation, accompanied by premature mesoderm differentiation, resulted from conditional mutation of *Fgf4* and *Fgf8* using T-Cre (Naiche et al., 2011). The early lethality and complex phenotype of these mutants precludes a detailed study of the role of *Fgf4* and *Fgf8* in axial elongation.

We have produced double mutants lacking both *Fgf4* and *Fgf8* expression in the primitive streak beginning at about E8.5. Loss of expression of both FGF family members in the posterior embryo causes severe defects in the formation of paraxial mesoderm. Although these mutants are able to survive until birth, vertebral condensations and ribs are disorganized and reduced in size or completely absent, and the neural tube is truncated in the lumbar region. The ability to allow FGF function during early gastrulation, followed by restricted gene inactivation has uncovered additional novel roles for signaling by FGF4 and FGF8 in late gastrulation.

Materials and methods

Mice

The *Fgf4* and *Fgf8* conditional and null alleles (Boulet et al., 2004; Moon et al., 2000; Moon and Capecchi, 2000), and the *hoxb1-IRES-Cre*

driver (Arenkiel et al., 2003) were previously described. Skeleton preparations were performed as previously described (Boulet and Capecchi, 2004). Development of appendicular skeletal structures was affected because the *hoxb1-IRES-Cre* driver reduces *Fgf4* and *Fgf8* expression in the AER of the limb bud.

Whole mount in situ hybridization and immunofluorescence

Whole mount in situs were performed as previously described (Boulet and Capecchi, 1996), except that proteinase K digestion was omitted and post hybridization washes were with 50% formamide, 2X SSC, 1% SDS without RNAse treatment for embryos from E8.5-E9. Template plasmids for riboprobe preparation were generated in the Capecchi lab (*Fgf4*, *Fgf8*, *Raldh2*, *Mesp2*, *Uncx4.1*, *Cyp26A1*) or kindly provided by C. Murtaugh (*mNotch1*), D. Wu (*Lfng*), B. Herrmann (*Brachyury*), S. Arber (*Etv4*), T. Gridley (*snail*), or A. McMahon (*Wnt3a* and *Shh*). Whole mount in situ-stained embryos were re-fixed, embedded in paraffin by standard protocols, sectioned and mounted in Fluormount G (Southern Biotech).

Immunofluorescence was performed on 10 μm cryosections. Antibodies used were anti-E-cadherin (SIGMA), anti-Brachyury (N19, Santa Cruz), anti-pHH3 (Upstate Biotechnology), and anti-laminin (SIGMA). Secondary antibodies were conjugated with Alexa fluor 488, 546 or 594 (Molecular Probes). TUNEL assay was performed using the In Situ Cell Death Detection kit (TMR red, Roche). Whole mount TUNEL assays were performed as previously described (Stadler et al., 2001).

Results

Conditional inactivation of Fgf4 and Fgf8 using hoxB1-IRES-Cre causes posterior truncation

To gain insight into the roles of *Fgf4* and *Fgf8* in posterior development, the *hoxB1-IRES-Cre* driver (*B1iCre*) (Arenkiel et al., 2003) was used to inactivate conditional alleles of *Fgf4* and *Fgf8* in posterior regions of the embryo. In crosses of *B1iCre* to the *ROSA26-lacZ* reporter, X-gal staining was first detected in the caudal primitive streak at E7 ((Arenkiel et al., 2003), Supplementary Fig. 1).

When *B1iCre* was used to inactivate *Fgf4* and *Fgf8*, noticeable decreases in the amount of *Fgf4* and *Fgf8* mRNAs in the posterior expression domains were detectable by E8.5 to E8.75 (Fig. 1A, B, G–J). By E9 to E9.5, *Fgf4* and *Fgf8* transcripts were essentially undetectable in the tail ectoderm and nascent mesoderm (Fig. 1C–F, K and L). *Fgf8* transcripts were still present in a small region corresponding to the hindgut at E9.5 (Fig. 1E and F; Supplementary Fig. 2).

We verified the reduction in FGF signaling in mutant embryos by examining the expression of the FGF target gene *Etv4*. *Etv4* gene expression was noticeably reduced at E8.5 and E8.75, and absent from the tail region of $Fgf4^{c/null}$; $Fgf8^{c/null}$; $hoxb1^{IRESCre/+}$ (*F4/F8/B1iCre*) mutant embryos by E9.5 (Fig. 1M–T).

Inactivation of only the *Fgf8* gene in the *hoxB1* domain did not result in any visible defect in axial elongation or vertebral morphology, in agreement with previously published data (Perantoni et al., 2005). Similarly, embryos with a conditional deletion of only *Fgf4* in the *hoxB1* domain appeared normal. In contrast, *F4/F8/B1iCre* double mutant embryos exhibit striking defects in posterior development. Mutant embryos at E9.5 could be distinguished from their litter mates by shorter tails and a reduced number of somites (Fig. 2A and B) and at E11.5, by a severely truncated tail (Fig. 2E and F). *F4/F8/B1iCre* mutant embryos at E15.5 completely lacked a tail (Fig. 2G and H). *Wnt5b* expression marks the most caudal region of the embryo at E10.5, including tail bud mesenchyme, the caudal neuropore and the caudal hindgut (Gofflot et al., 1997). Wnt5b expression is undetectable in E10.5 *F4/F8/B1iCre* mutant embryos (Fig. 2C and D).

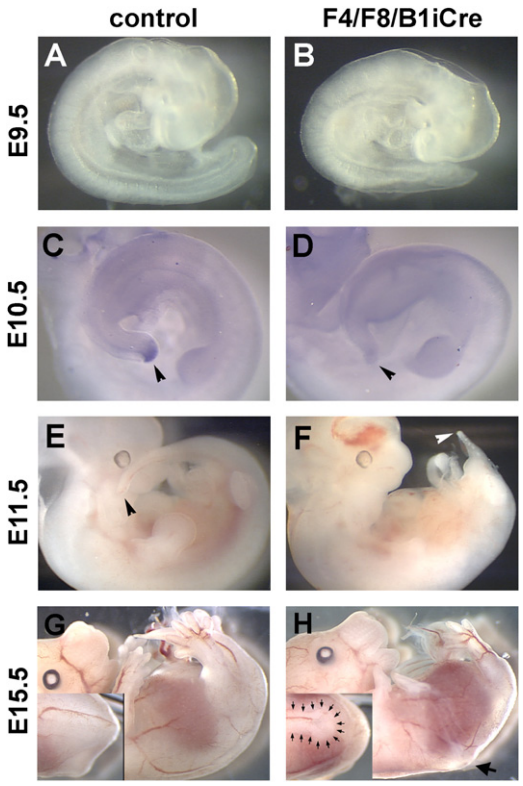

Fig. 2. *F4/F8/B1iCre* embryos show obvious morphological defects and loss of Wnt5b expression in the tail. E9.5 control (A) and double mutant (B) embryos. E10.5 control (C) and *F4/F8/B1iCre* mutant (D) embryos hybridized with a *Wnt5b* probe. Control (E) and double mutant (F) embryos at E11.5. Arrowheads point to the tip of the tail in (C), (D), (E), and (F). E15.5 control (G) and double mutant (H) embryos. Insets in (G) and (H) are higher magnification dorsal views of the lumbar region showing truncation of the neural tube in the mutant (H inset). Large arrow in (H) marks the level of neural tube truncation. Small arrows in (H inset) outline the posterior end of the neural tube.

In spite of the dramatic reduction in the development of posterior structures during gestation, mutant embryos survived until birth. Although cervical vertebrae formed normally, the thoracic skeleton showed multiple defects (Fig. 3A, C–E, G and H). The number of ribs was reduced from 13 to 7 or 8, with only 6 vertebrosternal ribs instead of 7 (Fig. 3C, D, G and H). The rib cage was reduced in size and abnormal in shape, and the ribs projected from the vertebral bodies at a peculiar angle (Fig. 3C and G). A partial transformation of T1 to C7 was observed in mutants, and the T1 rib often failed to reach the sternum instead fusing to the T2 rib in some cases (Fig. 3G; data not shown). Only remnants of the lumbar and sacral vertebrae were observed and no caudal tail vertebrae were present (Fig. 3A, B, E and F). Since AER expression of *Fgf4* and *Fgf8* is partially removed by *hoxB1-IRES-Cre*, limb development is affected in the mutants with variable expressivity (Fig. 2F and H).

Mutations that cause alterations in the distribution of retinoic acid (RA) or activity of the retinoic acid pathway affect axial skeletal development and rostral-caudal identity of vertebral elements (Lohnes et al., 1994). In particular, treatment of pregnant mice at 9.5 days of gestation with RA can cause severe axial truncations (Shum and Copp, 1996; Shum et al., 1999), and mutations in the RA-metabolizing cytochrome P450, *Cyp26A1*, cause tail truncations (Abu-Abed et al., 2001; Sakai et al., 2001). To determine whether an alteration in the retinoic acid pathway could contribute to the phenotype of *F4/F8/B1iCre* mutant

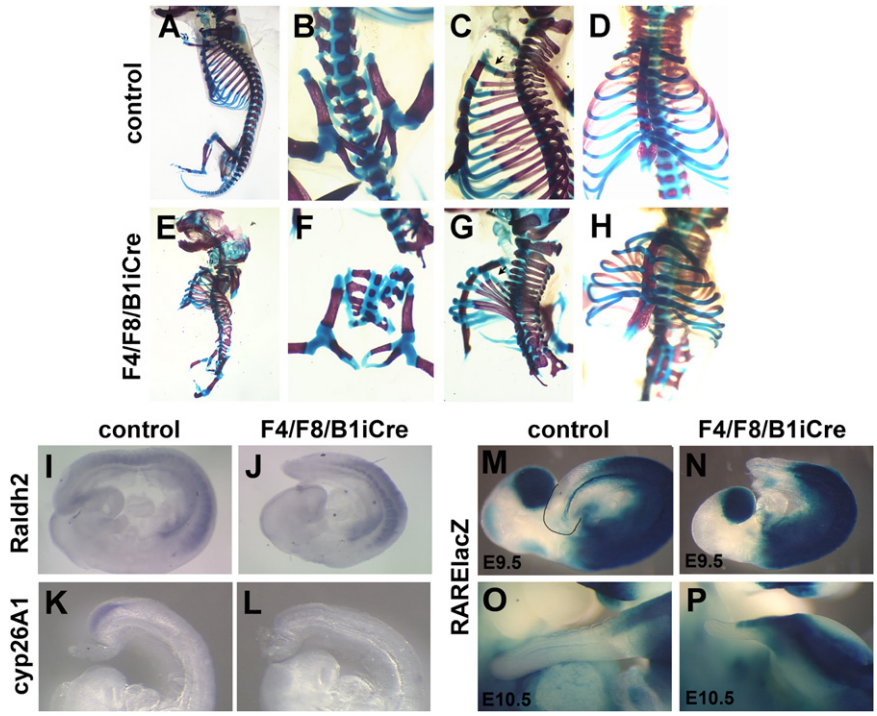

Fig. 3. *F4/F8/B1iCre* mutants show severe skeletal defects and reduction of Cyp26A1 expression. Skeleton preparations of control (A–D) and *F4/F8/B1iCre* mutant newborns (E–H). (B and F) Higher magnification ventral views of lumbar/sacral region. Lateral views (C and G) and ventral views (D and H) of thoracic region. (I and J) Whole mount in situ hybridization with a *Raldh2* probe to control (I) and *F4/F8/B1iCre* mutant (J) E9.5 embryos. (K and L) Expression of the *Cyp26A1* gene in control (K) and *F4/F8/B1iCre* mutant (L) E9 embryos. (M–P) X-gal stained E9.5 control (M), E9.5 mutant (N), E10.5 control (O) and E10.5 mutant (P) embryos carrying the RARE-lacZ transgene for detection of endogenous RA activity.

embryos, we examined the expression of *Cyp26A1* and *Raldh2*. The expression pattern of *Raldh2*, the primary RA-synthesizing enzyme, did not show expansion into posterior regions of the mutant embryo (Fig. 3I and J), but the expression of *Cyp26A1* was undetectable in mutant embryos by E9 (Fig. 3K and L). The level of retinoic acid signaling in the posterior embryo was examined using the RA activity reporter RARE-lacZ. At E9.5, the posterior limit of endogenous RA activity in mutant embryos was slightly closer to the tip of the tail than in the control, but at approximately the same position with respect to somite number, (Fig. 3M and N). At E10.5, although the area lacking RA activity is reduced in mutant embryos due to the reduced tail length (Fig. 3O and P), the posterior border is just caudal to the hindlimb buds as in the control, and there is still clearly a zone that lacks RA activity.

Development of the neural tube was abnormal in *F4/F8/B1iCre* mutants. The neural tube often had a twisted appearance as early as E8.5 (data not shown), and H&E stained sections revealed abnormal morphology at E9.5 and E10.5 (Fig. 6B, D and D'). The neural tube was truncated in E15.5 mutant embryos in the posterior thoracic or lumbar region (Fig. 2H).

Paraxial mesoderm production in the late primitive streak requires signaling by Fgf4 and Fgf8

Although *Fgf8* is required during early gastrulation for migration of mesoderm precursors away from the primitive streak (Sun et al., 1999), loss of only *Fgf8* at later stages does not affect the production of mesoderm (Perantoni et al., 2005). However, with the additional loss of *Fgf4* in *F4/F8/B1iCre* mutant embryos, the generation of paraxial mesoderm is increasingly affected as the body axis extends. Although rostral regions of mutant embryos at E9.0 (13 somite stage) show apparently normal somite formation (Fig. 4A and B), in more caudal regions, somites that do form are smaller or misshapen due to a progressive reduction in paraxial mesoderm (Fig. 4C–F), and a reduced amount of presomitic mesoderm is apparent in more posterior sections (Fig. 4G–N). Strikingly, the width of the primitive streak/neural plate of mutant embryos was greatly reduced compared to control embryos (Fig. 4I–N).

In *F4/F8/B1iCre* mutants, the first 12–13 somites showed characteristic stripes of *Uncx4.1* expression in the posterior compartment of each somite (Fig. 4O and P). In contrast, stripes of *Uncx4.1* expression in the more caudal paraxial region were irregularly spaced and often reduced in medial–lateral width (Fig. 4O–R). Some of the stripes appeared closer together, but in other cases, stripes were more widely separated, giving the appearance of an enlarged somite. In a few mutant embryos, posterior *Uncx4.1* stripes were asymmetrically positioned on each side of the neural tube (Fig. 4R), and in some cases *Uncx4.1* expression was seen at the midline at the most posterior end of the tail (Fig. 4T). The PSM of control embryos corresponds to the region between the most posterior Uncx4.1 stripe and the tip of the tail. Uncx4.1 expression in the mutants extends almost to the tip of the tail, indicating that the amount of PSM is severely decreased.

The expression of the PSM markers *Tbx6* and *Msgn1* was examined by whole mount in situ hybridization to visualize the extent of mesoderm loss in mutant embryos (Fig. 4U–Z). Severe reduction in the levels of *Tbx6* and *Msgn1* throughout the posterior end was observed, suggesting either a drastic reduction in the amount of PSM or a loss of PSM identity or both.

Reduction in expression of Brachyury and Wnt3a in F4/F8/B1iCre mutants

The *Wnt3a* and *Brachyury* gene products are required for continuous elongation of the embryonic axis (Beddington et al., 1992; Takada et al., 1994). In homozygous *Brachyury* mutants,

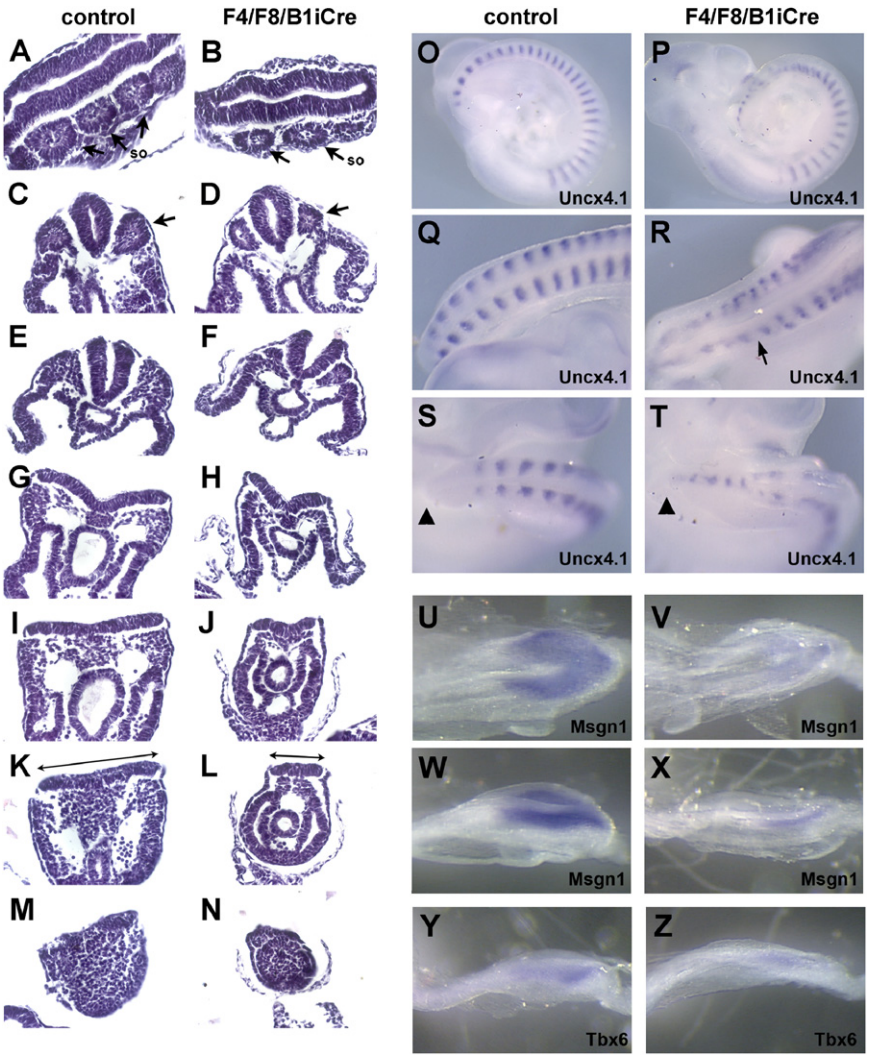

Fig. 4. Reduction in paraxial mesoderm and segmentation defects in *F4/F8/B1iCre* mutant embryos. H&E-stained longitudinal (A and B) or transverse (C–N) sections of control (A, C, E, G, I, K and M) and *F4/F8/B1iCre* mutant (B, D, F, H, J, L and N) embryos at E9 (13 somite stage). Arrows in (A–D) point to somites (so). Lines in (K) and (L) highlight difference in epiblast width between control and double mutant. (O, Q and S) Whole mount in situ hybridization of the *Uncx4.1* probe to control E9.5 embryos. (P, R and T) Expression of *Uncx4.1* in *F4/F8/B1iCre* mutant E9.5 embryos. (O and P) Lateral views and (Q–T) dorsal views of posterior embryo at higher magnification. Arrow in (R) points to region where *Uncx4.1* stripes are asymmetric. Arrowheads in (S and T) mark the tip of the tail. (U–X) *Msgn1* expression in E8.5 control (U and W) and *F4/F8/B1iCre* mutant (V and X) embryos. (U and V) Dorsal views and (W and X) dorsal-lateral views of primitive streak region. (Y and Z) Expression of *Tbx6* in control (Y) and *F4/F8/B1iCre* mutant (Z) embryos at E8.5.

development rostral to the forelimb appears normal, but in more caudal regions of the embryo, the notochord is absent and the neural tube and somites are abnormal ((Beddington et al., 1992) and references therein). *Wnt3a* null mutants are truncated rostral to the hindlimb and have a kinked neural tube (Takada et al., 1994). *Wnt3a* hypomorphs ($Wnt3a^{vt/vt}$) lack caudal vertebrae while $Wnt3a^{null/vt}$ embryos are truncated within the lumbar region (Greco et al., 1996).

When *Brachyury* expression was examined by whole mount in situ hybidization, reduced staining was seen lateral to the primitive streak in E8.5 *F4/F8/B1iCre* mutants relative to control embryos (Fig. 5A and B). At E9.5, there was a significant reduction in the amount of *Brachyury* mRNA detectable in the tail tip whereas notochord expression was not reduced (Fig. 5C and D). To investigate the reduced *Brachyury* signal in more detail, we used an anti-Brachyury antibody to examine protein expression in 9–10 somite stage embryos. Expression of Brachyury protein in the notochord was unaffected by the reduction in posterior FGF signaling in mutant embryos (Fig. 5E,F). In contrast, *F4/F8/B1iCre* embryos had significantly fewer Brachyury-expressing nascent mesoderm cells in the tail region (Fig. 5G and H).

Because several aspects of the *F4/F8/B1iCre* phenotype resembled that of *Wnt3a* null and hypomorphic mutants, we examined the expression of *Wnt3a*. In control embryos at E8.5, *Wnt3a* is expressed in the primitive streak in the ectodermal layer, but not in the migrating mesoderm cells, while *Wnt3a* transcripts are detected at the very tip of the tail at E9.5 ((Yoshikawa et al., 1997), Fig. 5I and K). In *F4/F8/B1iCre* mutant embryos, the level of *Wnt3a* expression was already noticeably reduced at E8.5 (Fig. 5J). By E9.5, little or no *Wnt3a* expression could be detected in the tail while expression in the brain and spinal cord was unaffected (Fig. 5L).

Abnormal neural tube development in F4/F8/B1iCre mutants

In *Wnt3a* null embryos, cells which have ingressed through the primitive streak do not migrate laterally, but instead remain under the streak and form ectopic neural tube-like structures

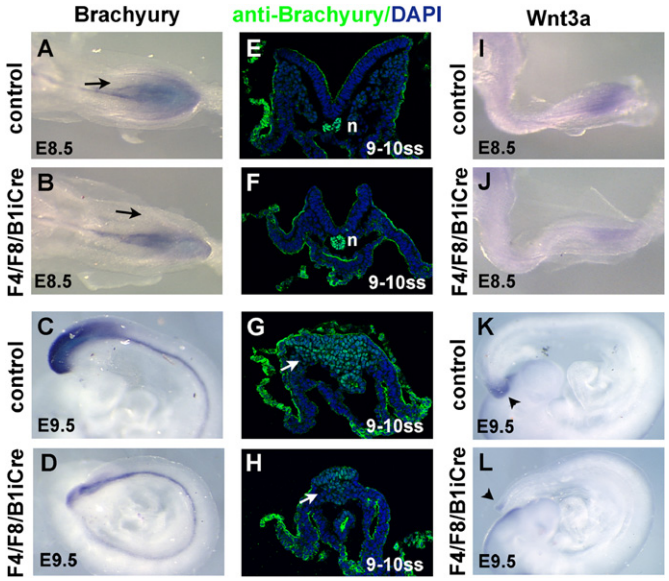

Fig. 5. Expression of *Brachyury* and *Wnt3a* in *F4/F8/B1iCre* mutant embryos. (A–D) Whole mount in situ hybridization of E8.5 control (A), E8.5 *F4/F8/B1iCre* mutant (B), E9.5 control (C) and E9.5 mutant (D) embryos with a *Brachyury* probe. Black arrows in (A) and (B) point to nascent mesoderm emerging from the primitive streak. (E–H) Immunofluorescence of control (E and G) and mutant (F and H) cryosections of 9–10 somite stage embryos stained with an anti-Brachyury antibody (green). The anti-Brachyury antibody gives backgound staining in epithelial tissues which is readily distinguished from the nuclear Brachyury staining. Sections were counterstained with DAPI (blue). White arows point to nascent mesoderm beneath the primitive streak expressing Brachyury protein. n, notochord. (I–L) Expression of *Wnt3a* in E8.5 control (I), E8.5 *F4/F8/B1iCre* mutant (J), E9.5 control (K), and E9.5 mutant (L) embryos. Arrowheads in (K) and (L) point to expression of *Wnt3a* in the tail.

(Yoshikawa et al., 1997). Furthermore, *Fgfr1*-null cells form ectopic neural tubes in chimeric embryos (Ciruna et al., 1997). In *F4/F8/B1iCre* mutant embryos at E9.5 and E10.5, structures that appear to be secondary neural tubes can be detected in H&E-stained sections (Fig. 6A–D'). Anti-Sox2 antibody staining of cryosections of control and mutant E9.5 embryos showed ectopic Sox2 expression in structures resembling secondary neural tubes in the posterior embryo (Fig. 6J). At 11.5, *Sox2* whole mount in situ hybridization showed expanded posterior neural tissue, curvature of the spinal cord and occasional failure of neural tube closure (Fig. 6K–N; data not shown). Similar to RA-treated embryos (Shum et al., 1999), which have a reduction in the level of *Wnt3a*, *F4/F8/B1iCre* mutant spinal cords were truncated at a position anterior to the hind limbs at E15.5, and an expanded loop of neural tissue was observed at the posterior end (Fig. 2H). Ectopic neural tubes were not detected histologically at E13.5, although the posterior neural tube of mutant embryos showed abnormal morphology (Fig. 6F) in comparison to the characteristic structure seen in the control (Fig. 6E).

Posterior notochord expansion revealed by Shh expression

When the production of FGFR1alpha isoforms was specifically disrupted in the mouse, posteriorly directed axial mesoderm migration did not occur, resulting in a failure to form the posterior notochord and truncation of mutant embryos (Xu et al., 1999). The notochord was examined in *F4/F8/B1iCre* mutant embryos using whole mount in situ hybridization with a *Shh* probe. In E9.5 mutant embryos, the *Shh* expression pattern indicated that anterior notochord formation was undisturbed (Fig. 6O and P). In E10.5 mutant embryos there was no evidence of a failure to form posterior notochord, but rather an expansion of the most caudal *Shh*-expressing tissue (Fig. 6Q and R). In sections of whole mount in situ-stained E10.5 embryos, *Shh* appeared to be expressed in two notochords at some levels, both associated with the primary neural tube (Fig. 6S and T).

Expression of Notch, Lunatic fringe and Mesp2

FGF signaling plays a critical role in segmentation of the vertebrate embryo (Dubrulle et al., 2001; Dubrulle and Pourquie, 2004; Naiche et al.; Wahl et al., 2007). In the clock and wavefront model, the wavefront appears to be established by opposition of the posterior activity of WNT and FGF/MAPK pathways and rostral retinoic acid pathway activity (Wahl et al., 2007). A recent study using conditional ablation of *Fgfr1* in the PSM showed that FGF signaling is required for oscillating gene expression and somite formation, acting upstream of the NOTCH and WNT pathways (Wahl et al., 2007). Expression of *Notch1*, *Lunatic fringe* (*Lfng*) and *Mesp2* were examined in *F4/F8/B1iCre* embryos to investigate the role of the FGF4 and FGF8 ligands in the control of the segmentation clock.

Mesp2 is expressed in a single stripe in the rostral PSM in the region that will form the next somite and is downregulated immediately after somite formation. At E8.5-8.75, weak stripes of *Mesp2* expression were detectable in mutant embryos (Fig. 7A and B). *Mesp2* expression was undetectable in *F4/F8/B1iCre* mutant embryos at E9-9.5 (Fig. 7C and D; 4/4 controls and 0/5 mutants showed *Mesp2* stripes).

Lunatic fringe (*Lfng*) is expressed in the presomitic mesoderm in an oscillating pattern. In the presomitic mesoderm of *F4/F8/B1iCre* mutant embryos, only extremely low levels of *Lfng* transcripts were detectable, even in the youngest embryos examined (E8.75), and the weak expression pattern did not resemble any stage of the normal oscillating pattern (Fig. 7G–L).

Expression of the *Notch1* gene and subsequent cleavage of the Notch receptor into the active form play a central role in embryo segmentation. In *Notch1* mutant embryos, somitogenesis ceases after the production of the first 14 somites (Conlon et al., 1995). In control embryos, *Notch1* transcripts are present at high levels in the anterior presomitic mesoderm, and at lower levels in the nervous system. In most *F4/F8/B1iCre* mutant embryos examined at E9-9.5, expression of *Notch1* was detected in a pattern similar to controls, but reflecting the reduced size of the PSM (Fig. 7E and F).

E-cadherin expression is down-regulated normally in the mutant primitive streak but epiblast width is drastically reduced

In *Fgfr1* mutants, *Snail* expression in the primitive streak is significantly reduced and, as in *Snail* mutants (Carver et al., 2001), *E-cadherin* expression is not down regulated, cells fail to undergo the EMT, and cannot migrate away from the streak (Ciruna and Rossant, 2001). Expression of *Snail* was examined by whole mount in situ hybridization. *Snail* expression could be detected in the presomitic mesoderm of E8.5 mutant embryos although the level of expression appeared significantly lower than that of controls (Fig. 8A and B). At E9, the level of *Snail* transcripts was decreased in mutant embryos and the pattern of expression did not resemble any of the phases of cyclic *Snail* expression seen in wild type embryos (Dale et al., 2006) (Fig. 8C and D). Although *Snail* expression appears to be decreased, extensive cell accumulation beneath the primitive streak or at the tail end of the embryo was not observed in *F4/F8/B1iCre* mutant embryos between the 4 and 10 somite stage (Fig. 5H, Fig. 8F, H and J).

To test whether the paraxial mesoderm defects in *F4/F8/B1iCre* mutants could be due to a failure to down regulate E-cadherin at the late primitive streak, cryosections of E8.5 to E9 *F4/F8/B1iCre*

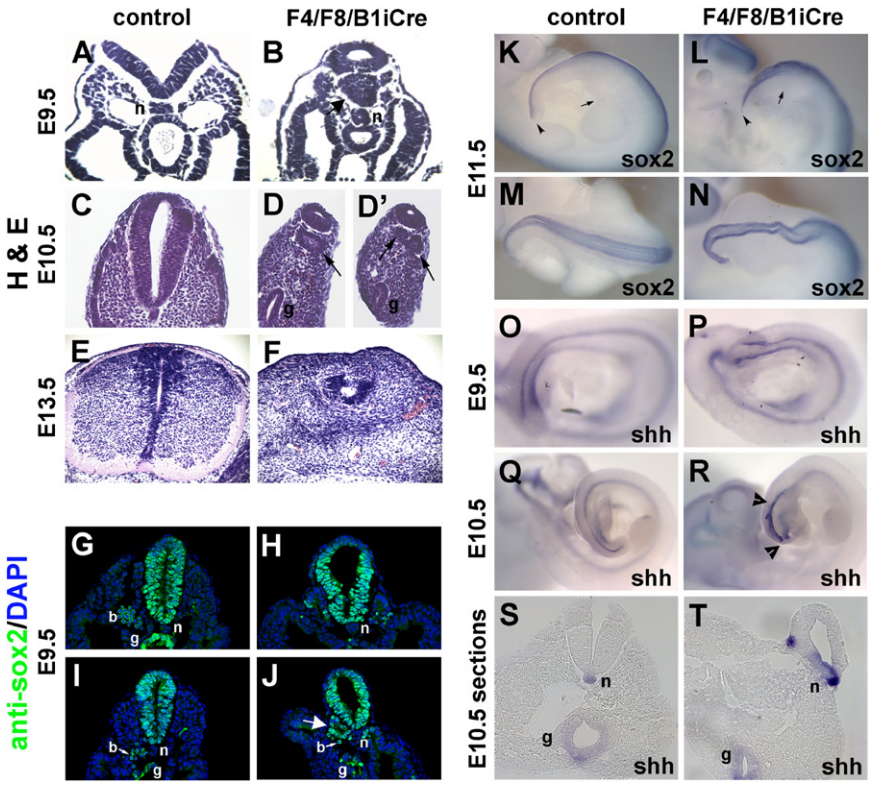

Fig. 6. Neural tube and notochord abnormalities in *F4/F8/B1iCre* mutants. (A–F) H&E-stained paraffin sections of E9.5 control (A), E9.5 *F4/F8/B1iCre* mutant (B), E10.5 control (C), E10.5 mutant (D, D'), E13.5 control (E), and E13.5 mutant (F) embryos. Arrows in (B), (D) and (D') mark structures resembling ectopic neural tubes. (G–J) Sox2 protein expression in cryosections of control (G and I) and *F4/F8/B1iCre* mutant (H and J) E10.5 embryos. Large white arrow in (J) points to structure resembling an ectopic neural tube. Small white arrows in (I and J) point to blood cells (b). n, notochord; g, hindgut. (K–N) *Sox2* expression in E11.5 control (K and M) and E11.5 *F4/F8/B1iCre* mutant (L and N) embryos. (K and L) lateral views and (M and N) dorsal views of tail region. Small arrows in (K) and (L) point to posterior edge of hind limb bud and arrowheads point to tip of the tail. (O–R) *Shh* expression in E9.5 (O) and E10.5 (Q) control embryos and E9.5 (P) and E10.5 (R) *F4/F8/B1iCre* mutant embryos. Arrowheads in (R) delimit expanded region of *Shh* expression. (S and T) Sections from whole mount E10.5 control (S) and mutant (T) embryos hybridized with the *Shh* probe.

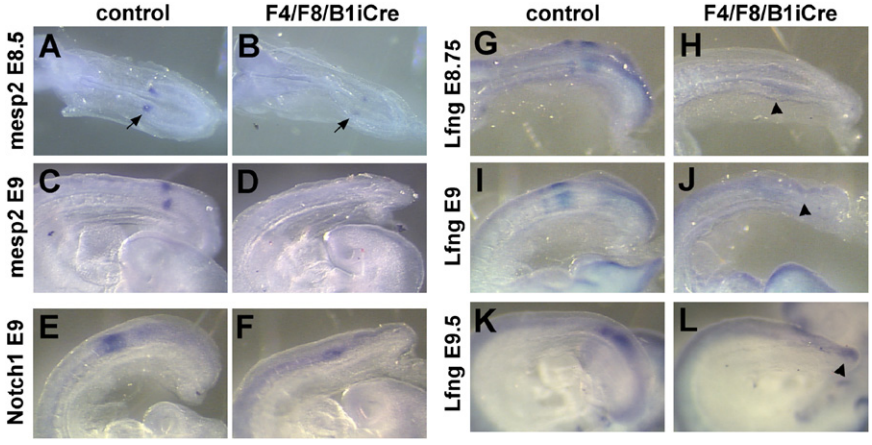

Fig. 7. Expression of segmentation clock components is altered in *F4/F8/B1iCre* mutant embryos. (A–D) Whole mount in situ hybridization of E8.5 control (A) and *F4/F8/B1iCre* mutant (B), and E9 control (C) and mutant (D) embryos with the *Mesp2* probe. Arrows in (A) and (B) point to stripes of *Mesp2* expression. (E and F) *Notch1* expression in E9 control (E) and E9 mutant (F) embryos. (G–L) Expression of *Lunatic fringe* (*Lfng*) in E8.75 control (G), E8.75 mutant (H), E9 control (I), E9 mutant (J), E9.5 control (K) and E9.5 mutant (L) embryos. Arrowheads in (H), (J), and (L) point to regions of weak *Lfng* expression in *F4/F8/B1iCre* mutants.

mutant embryos were stained with an anti-E-cadherin antibody. We were unable to detect any evidence of ectopic E-cadherin expression in cells at the primitive streak in embryos at the 7 somite stage (Fig. 8E–H). Furthermore, anti-laminin staining of the primitive streak region at the 8 somite stage indicates that cells continue to ingress through the primitive streak in mutant embryos (Fig. 8I and J). The anti-laminin antibody stains the basement membrane separating epiblast from mesoderm, and a gap in laminin marks the position of the primitive streak. Since six prospective somites are present in the mouse PSM (reviewed in (Pourquie, 2001)), the precursors of somites 13–14 should be exiting the primitive streak of 7–8 somite stage embryos, and a defect in mesoderm production at the primitive streak should be visible in *F4/F8/B1iCre* mutant embryos by this stage.

The tail region, consisting of late primitive streak and precursors of the posterior spinal cord, of 13 somite stage *F4/F8/B1iCre* mutant embryos was considerably narrower than that of control embryos (Fig. 4I–N). A significant reduction in epiblast

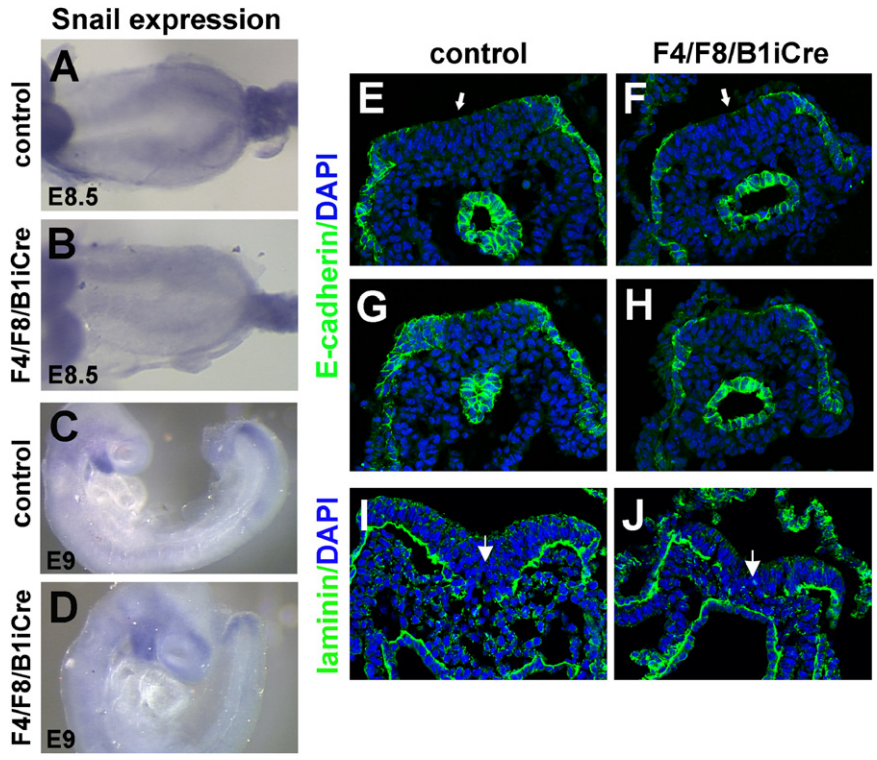

Fig. 8. Expression of *Snail* mRNA and E-cadherin protein in *F4/F8/B1iCre* mutant embryos. (A–D) *Snail* expression in E8.5 control (A), E8.5 mutant (B), E9 control (C) and E9 mutant (D) embryos hybridized with a *Snail* probe. (E–H) Anti-E-cadherin antibody (green) staining of cryosections of control (E and G, rostral to caudal) and *F4/F8/B1iCre* mutant (F and H, rostral to caudal) embryos at the 7 somite stage with DAPI counterstain (blue). (I and J) Anti-laminin staining (green) of sections from control (I) and mutant (J) embryos at the 8 somite stage, counterstained with DAPI (blue). White arrows mark the primitive streak region.

width was seen in 9–10 somite stage mutant embryos relative to controls (Fig. 5G and H), and a slight reduction was detectable in some mutant embryos at the 7–8 somite stage (Fig. 8G–J). To more carefully examine the change in epiblast width, mutant and control embryos at the 4 to 8 somite stage were collected. Embryos were matched by somite number as well as by size. Embryos were stained with anti-laminin and anti-brachyury antibodies to aid in identification of the primitive streak and the node. In most cases, the area of the epiblast was significantly smaller in the mutant embryo than in the control, from the node region to the posterior end (Supplementary Fig. 3). Size differences were more striking at a greater distance from the node and in older embryos.

Apoptosis and proliferation are not altered in F4/F8/B1iCre mutants

The progressive reduction in the amount of paraxial mesoderm produced in *F4/F8/B1iCre* mutant embryos could be due to reduced cell proliferation, increased cell death, failure to maintain a stem cell population, aberrant differentiation of prospective paraxial mesoderm cells, or a combination of some or all of these factors. As a reduction in the width of the epiblast was obvious by about the 10 somite stage, cell proliferation was measured in embryos at a slightly earlier time point (6–7 somite stage) by counting phospho-histone H3-positive cells. In mutant embryos at the 6–7 somite stage, no reduction in percentage of phh3-positive cells in the primitive streak/epiblast could be detected (Supplementary Table 1).

Fgf4 and *Fgf8* are required for cell survival in the developing limb buds, and increased apoptosis correlates with the lack of limb skeletal elements in mice lacking AER expression of these FGF ligands (Boulet et al., 2004; Sun et al., 2002). A cell survival role has also been demonstrated for *Fgf8* in midbrain and forebrain development (Chi et al., 2003; Storm et al., 2006), differentiation of pharyngeal arch-derived structures (Frank et al., 2002; Macatee et al., 2003), and kidney development (Grieshammer et al., 2005; Perantoni et al., 2005). However, no increase in apoptosis in the primitive streak of *F4/F8/B1iCre* mutant embryos could be detected prior to the appearance of mesoderm reduction (Supplementary Table 1).

Discussion

The loss of signaling by FGF4 and FGF8 during late gastrulation severely curtails the further production of paraxial mesoderm in *F4/F8/B1iCre* mutant embryos. Although mesoderm precursors fail to migrate away from the primitive streak in *Fgf8* or *Fgfr1* null mutants, this does not appear to be the case when signaling by FGF4 and FGF8 is lost during late gastrulation. In *F4/F8/B1iCre* mutants, there is no evidence for failure to down-regulate E-cadherin expression at the primitive streak that would lead to inability of the cells to undergo EMT, nor is there noticeable accumulation of cells that are unable to migrate away from the primitive streak. Instead, the primary defect appears to be a progressive reduction in the width of the primitive streak ectoderm or epiblast, leading to a reduction in precursors for paraxial mesoderm. Interestingly, the presence of hindlimbs in *F4/F8/B1iCre* mutants indicates that the production of lateral mesoderm is not as strongly affected as paraxial mesoderm. This correlates with the ability of *Fgfr1* mutant cells in chimeras to contribute effectively to lateral mesoderm, but not paraxial mesoderm (Ciruna et al., 1997). Likewise, the presence of kidneys in *F4/F8/B1iCre* mutant embryos establishes that at least some derivatives of intermediate mesoderm are also produced (data not shown).

Despite the decreased epiblast size, we were unable to detect alterations in cell proliferation or apoptosis. It is possible that changes in proliferation rate or apoptosis occur during a very short time interval that was not sampled in our study. Stem cells may occupy only a small region of the epiblast such that loss of self-renewing divisions would not be readily detectable. Although there was some abnormal differentiation of mesoderm cells into neural tissue as well as expanded axial mesoderm, this does not account for the overall reduction in posterior tissue produced nor does it explain the reduction in epiblast size. There is accumulating experimental evidence in mouse and chick that axial tissues of the embryo are derived from stem cells (reviewed in (Tzouanacou et al., 2009; Wilson et al., 2009)). Cambray and Wilson, 2007 have shown that cells from the E8.5 mouse embryo node-streak border and ectoderm lateral to the primitive streak contribute to the developing axis and to the chordoneural hinge (CNH) in the tail bud of E10.5 embryos. The CNH has been shown to contain long-term axial progenitors capable of contributing to both mesodermal and neural tissues, which therefore show stem cell-like properties (Cambray and Wilson, 2002). FGF signaling may be required for the maintenance of a stem cell population in the epiblast. In the absence of FGF4 and FGF8, stem cells would not be renewed and the supply of epiblast cells that undergo EMT, ingress through the primitive streak and become paraxial mesoderm is prematurely exhausted.

The expression patterns of *Brachyury* and *Wnt3a*, two key genes required for posterior elongation of the mouse embryo, were dramatically affected in *F4/F8/B1iCre* mutants. The nascent mesoderm cells which express *Brachyury* were progressively eliminated while epiblast and notochord cells continue to express the gene. FGF signaling via FGF4 and FGF8 is therefore required for the production of *Brachyury*-expressing mesoderm cells at the primitive streak, but does not appear to be required for *Brachyury* expression in the epiblast or the notochord.

Wnt3a mutant embryos appear superficially similar to the *F4/F8/B1iCre* mutants in that *Wnt3a* mutants show significant narrowing of the primitive streak by the 10 somite stage and have a shortened axis at E9.5 (Takada et al., 1994). However, *Wnt3a* null mutants lack somites posterior to the forelimb level (after about somite 9) and do not form any caudal structures while *F4/F8/B1iCre* mutants have ventral posterior mesoderm-derived structures and hind limbs. *Wnt3a* expression in *Wnt3a* hypomorphs (*vt/vt*) is barely detectable in the tail bud at E9.5 similar to *F4/F8/B1iCre* mutants. However, *Notch* and *Lunatic fringe* expression in the tail region is maintained in *vt/vt* embryos in the absence of detectable *Wnt3a* expression (Aulehla et al., 2003). Therefore, the phenotype obtained upon loss of FGF4/FGF8 signaling during late gastrulation does not simply recapitulate the phenotype caused by loss or severe reduction of *Wnt3a* expression.

Wnt3a mutants and *Tbx6* mutants show differentiation of presumptive mesoderm into ectopic neural tissue (Chapman and Papaioannou, 1998; Yoshikawa et al., 1997). Similarly, *F4/F8/B1iCre* mutant embryos appear to have ectopic neural tubes. The patches of *Sox2*-positive cells indicate that a small number of mesodermal cells have taken on a neural fate. In the same way, expansion of the *Shh*-expressing tissue could be the result of continued production of axial progenitors without adequate elongation of the axis.

WNT signaling is required for *Fgf8* expression during gastrulation: *Fgf8* expression is down-regulated in *β-catenin* mutant embryos at E6.5 (Morkel et al., 2003) and absent from E8.5 embryos in which *β-catenin* was inactivated in the primitive streak using *T-cre* (Dunty et al., 2008). In addition, *Fgf8* expression in the tail is significantly decreased in *Wnt3a* hypomorphs (*vt/vt*) at E10.25 (Aulehla et al., 2003). These observations strongly suggest that *Fgf8* is downstream of WNT signaling in the early embryo. On the other hand, *Wnt3a* expression is almost completely lost in *F4/F8/B1iCre* mutants. To some extent, this could be due to the loss of the posterior epiblast and nascent mesoderm in mutant embryos, the sites of strongest Wnt3a expression at the stages examined (Nowotschin et al. 2012).

Overall, the phenotypic similarities of mutants in the FGF and WNT signaling pathways and the complex regulatory relationship suggest that these two pathways act together in promoting elongation of the body axis. Recent studies in the mouse limb show that WNT and FGF signaling act synergistically to promote proliferation and maintain multipotent progenitor cells in an undifferentiated state (ten Berge et al., 2008). In a similar manner, these two signaling pathways may act together in body elongation to promote growth while maintaining a stem cell population in the epiblast.

In chick embryos, RA attenuates FGF signaling in the paraxial mesoderm and FGF signaling regulates RA synthesis in the paraxial mesoderm through an effect on the expression of *Raldh2* (Diez del Corral et al., 2003). In the mouse, *Raldh2*$^{-/-}$ embryos show an anterior shift in the expression of *Fgf8* and subsequently, asymmetric somite formation (Vermot et al., 2005). *Fgfr1* conditional mutants show a loss of *Cyp26A1* expression in the tail as seen in *F4/F8/B1iCre* embryos, but do not show an increase in RA activity as determined by use of the RARE-lacZ reporter or a posterior expansion of the *Raldh2* expression pattern at the stages examined (Wahl et al., 2007). Similarly, *F4/F8/B1iCre* mutants also do not show a posterior expansion of the *Raldh2* expression domain or RA activity, indicating that FGF signaling via FGF4 and FGF8 is not likely to be required to limit the extent of RA-synthesizing activity along the embryonic axis. A recent study of the role of RA signaling in the termination of body axis extension (Cunningham et al., 2011) shows that *Cyp26A1* expression in the tailbud at E10.5 or later is unnecessary for RA degradation. However, the contribution of the absence of *Cyp26A1* expression to the phenotype of *F4/F8/B1ic* mutants cannot be conclusively determined at this time.

In the clock and wavefront model of somitogenesis, the FGF8 protein gradient has been proposed to provide the wavefront, perhaps in concert with other factors, such as WNT3a. As the embryonic axis extends, cells in the anterior PSM are exposed to a decreasing level of FGF (Dubrulle and Pourquie, 2004). When the level of FGF signaling to which the cells are exposed falls below a threshold at the "determination front", the cells are no longer maintained in the undifferentiated state and are then able to respond to the segmentation clock and form somites. It is clear that FGF8 alone does not provide this function as segmentation proceeds normally in embryos in which *Fgf8* expression has been eliminated from the posterior embryo (Perantoni et al., 2005). FGF4 is able to partially compensate for the absence of FGF8 in the AER during limb bud development (Lewandoski et al., 2000; Moon and Capecchi, 2000), and may similarly compensate for the absence of FGF8 in posterior development of the embryo. Indeed, double *Fgf4/Fgf8* mutants described in this study show severe defects in embryo elongation, and are clearly required for proper expression of segmentation clock genes as shown previously for *Fgfr1* mutants (Wahl et al., 2007). However, due to the failure of these mutants to produce sufficient PSM for the continued production of somites, interpretation of the phenotype with respect to the role of FGFs in establishment of the determination front is very difficult. In a similar study in which *Fgf4* and *Fgf8* were inactivated by T-Cre rather than *hoxB1-IRES-Cre*, premature differentiation of the PSM was observed (Naiche et al., 2011). This supports a role for *Fgf4* and *Fgf8* in wavefront establishment.

In summary, the FGF signaling pathway plays multiple roles in axial elongation of the mouse embryo. The earliest role is in the epithelial to mesenchyme transition and subsequent cell

migration at the primitive streak (Ciruna and Rossant, 2001). *Fgf4* and *Fgf8* are subsequently required to maintain the expression of genes critical for paraxial mesoderm formation and the expression of segmentation clock genes, as well as for wavefront activity as described above (Naiche et al. 2011). The results of our study support and extend these findings, uncovering a later role of FGF signaling. *Fgf4* and *Fgf8* are required for the maintenance of stem or progenitor cells in the late gastrulation epiblast. Failure to maintain the epiblast layer results in a severe deficit in the production of paraxial mesoderm at the posterior end of the embryo, and the failure of stem cells to be incorporated in a tail bud structure, ultimately resulting in premature termination of axial elongation.

Acknowledgments

We thank Yuanyuan Wu for the Raldh2 probe, and Lisa Urness and Suzi Mansour, Charles Murtaugh, and Yukio Saijoh for providing additional probe templates and mouse strains. We also thank Nadja Makki for whole mount in situ hybridization protocols, and M. Hockin, Y. Saijoh, L.A. Naiche, M. Lewandoski, and K. Storey for comments on the manuscript. This work was supported by grants from the NIH (NIH2R01GM021168-37) and Howard Hughes Medical Institute to M.R.C.

Appendix A. Supporting information

Supplementary data associated with this article can be found in the online version at http://dx.doi.org/10.1016/j.ydbio.2012.08.017.

References

Abu-Abed, S., Dolle, P., Metzger, D., Beckett, B., Chambon, P., Petkovich, M., 2001. The retinoic acid-metabolizing enzyme, CYP26A1, is essential for normal hindbrain patterning, vertebral identity, and development of posterior structures. Genes Dev. 15, 226–240.

Arenkiel, B.R., Gaufo, G.O., Capecchi, M.R., 2003. Hoxb1 neural crest preferentially form glia of the PNS. Dev. Dyn. 227, 379–386.

Aulehla, A., Wehrle, C., Brand-Saberi, B., Kemler, R., Gossler, A., Kanzler, B., Herrmann, B.G., 2003. Wnt3a plays a major role in the segmentation clock controlling somitogenesis. Dev. Cell 4, 395–406.

Beddington, R.S., Rashbass, P., Wilson, V., 1992. Brachyury-a gene affecting mouse gastrulation and early organogenesis. Dev. Suppl., 157–165.

Boulet, A.M., Capecchi, M.R., 1996. Targeted disruption of hoxc-4 causes esophageal defects and vertebral transformations. Dev. Biol. 177, 232–249.

Boulet, A.M., Capecchi, M.R., 2004. Multiple roles of Hoxa11 and Hoxd11 in the formation of the mammalian forelimb zeugopod. Development 131, 299–309.

Boulet, A.M., Moon, A.M., Arenkiel, B.R., Capecchi, M.R., 2004. The roles of Fgf4 and Fgf8 in limb bud initiation and outgrowth. Dev. Biol. 273, 361–372.

Cambray, N., Wilson, V., 2002. Axial progenitors with extensive potency are localised to the mouse chordoneural hinge. Development 129, 4855–4866.

Cambray, N., Wilson, V., 2007. Two distinct sources for a population of maturing axial progenitors. Development 134, 2829–2840.

Carver, E.A., Jiang, R., Lan, Y., Oram, K.F., Gridley, T., 2001. The mouse snail gene encodes a key regulator of the epithelial-mesenchymal transition. Mol. Cell. Biol. 21, 8184–8188.

Chapman, D.L., Papaioannou, V.E., 1998. Three neural tubes in mouse embryos with mutations in the *T*-box gene Tbx6. Nature 391, 695–697.

Chi, C.L., Martinez, S., Wurst, W., Martin, G.R., 2003. The isthmic organizer signal FGF8 is required for cell survival in the prospective midbrain and cerebellum. Development 130, 2633–2644.

Ciruna, B., Rossant, J., 2001. FGF signaling regulates mesoderm cell fate specification and morphogenetic movement at the primitive streak. Dev. Cell 1, 37–49.

Ciruna, B.G., Schwartz, L., Harpal, K., Yamaguchi, T.P., Rossant, J., 1997. Chimeric analysis of fibroblast growth factor receptor-1 (Fgfr1) function: a role for FGFR1 in morphogenetic movement through the primitive streak. Development 124, 2829–2841.

Conlon, R.A., Reaume, A.G., Rossant, J., 1995. Notch1 is required for the coordinate segmentation of somites. Development 121, 1533–1545.

Cunningham, T.J., Zhao, X., Duester, G., 2011. Uncoupling of retinoic acid signaling from tailbud development before termination of body axis extension. Genesis 49, 776–783.

Dale, J.K., Malapert, P., Chal, J., Vilhais-Neto, G., Maroto, M., Johnson, T., Jayasinghe, S., Trainor, P., Herrmann, B., Pourquie, O., 2006. Oscillations of the snail genes in the presomitic mesoderm coordinate segmental patterning and morphogenesis in vertebrate somitogenesis. Dev. Cell 10, 355–366.

Dequeant, M.L., Glynn, E., Gaudenz, K., Wahl, M., Chen, J., Mushegian, A., Pourquie, O., 2006. A complex oscillating network of signaling genes underlies the mouse segmentation clock. Science 314, 1595–1598.

Diez del Corral, R., Olivera-Martinez, I., Goriely, A., Gale, E., Maden, M., Storey, K., 2003. Opposing FGF and retinoid pathways control ventral neural pattern, neuronal differentiation, and segmentation during body axis extension. Neuron 40, 65–79.

Diez del Corral, R., Storey, K.G., 2004. Opposing FGF and retinoid pathways: a signalling switch that controls differentiation and patterning onset in the extending vertebrate body axis. Bioessays 26, 857–869.

Dubrulle, J., McGrew, M.J., Pourquie, O., 2001. FGF signaling controls somite boundary position and regulates segmentation clock control of spatiotemporal Hox gene activation. Cell 106, 219–232.

Dubrulle, J., Pourquie, O., 2004. fgf8 mRNA decay establishes a gradient that couples axial elongation to patterning in the vertebrate embryo. Nature 427, 419–422.

Dunty Jr., W.C., Biris, K.K., Chalamalasetty, R.B., Taketo, M.M., Lewandoski, M., Yamaguchi, T.P., 2008. Wnt3a/beta-catenin signaling controls posterior body development by coordinating mesoderm formation and segmentation. Development 135, 85–94.

Frank, D.U., Fotheringham, L.K., Brewer, J.A., Muglia, L.J., Tristani-Firouzi, M., Capecchi, M.R., Moon, A.M., 2002. An Fgf8 mouse mutant phenocopies human 22q11 deletion syndrome. Development 129, 4591–4603.

Gofflot, F., Hall, M., Morriss-Kay, G.M., 1997. Genetic patterning of the developing mouse tail at the time of posterior neuropore closure. Dev. Dyn. 210, 431–445.

Greco, T.L., Takada, S., Newhouse, M.M., McMahon, J.A., McMahon, A.P., Camper, S.A., 1996. Analysis of the vestigial tail mutation demonstrates that Wnt-3a gene dosage regulates mouse axial development. Genes Dev. 10, 313–324.

Grieshammer, U., Cebrian, C., Ilagan, R., Meyers, E., Herzlinger, D., Martin, G.R., 2005. FGF8 is required for cell survival at distinct stages of nephrogenesis and for regulation of gene expression in nascent nephrons. Development 132, 3847–3857.

Lewandoski, M., Sun, X., Martin, G.R., 2000. Fgf8 signalling from the AER is essential for normal limb development. Nat. Genet. 26, 460–463.

Lohnes, D., Mark, M., Mendelsohn, C., Dolle, P., Dierich, A., Gorry, P., Gansmuller, A., Chambon, P., 1994. Function of the retinoic acid receptors (RARs) during development (I). Craniofacial and skeletal abnormalities in RAR double mutants. Development 120, 2723–2748.

Macatee, T.L., Hammond, B.P., Arenkiel, B.R., Francis, L., Frank, D.U., Moon, A.M., 2003. Ablation of specific expression domains reveals discrete functions of ectoderm- and endoderm-derived FGF8 during cardiovascular and pharyngeal development. Development 130, 6361–6374.

Moon, A.M., Boulet, A.M., Capecchi, M.R., 2000. Normal limb development in conditional mutants of Fgf4. Development 127, 989–996.

Moon, A.M., Capecchi, M.R., 2000. Fgf8 is required for outgrowth and patterning of the limbs. Nat. Genet. 26, 455–459.

Morkel, M., Huelsken, J., Wakamiya, M., Ding, J., van de Wetering, M., Clevers, H., Taketo, M.M., Behringer, R.R., Shen, M.M., Birchmeier, W., 2003. Beta-catenin regulates Cripto- and Wnt3-dependent gene expression programs in mouse axis and mesoderm formation. Development 130, 6283–6294.

Naiche, L.A., Holder, N., Lewandoski, M., 2011. FGF4 and FGF8 comprise the wavefront activity that controls somitogenesis. PNAS 108, 4018–23.

Niwa, Y., Masamizu, Y., Liu, T., Nakayama, R., Deng, C.X., Kageyama, R., 2007. The initiation and propagation of Hes7 oscillation are cooperatively regulated by Fgf and notch signaling in the somite segmentation clock. Dev. Cell 13, 298–304.

Nowotschin, S., Ferrer-Vaquer, A., Concepcion, D., Papaioannou, V.E., Hadjantonakis, A.K., 2012. Interaction of Wnt3a, Msgn1 and Tbx6 in neural versus paraxial mesoderm lineage commitment and paraxial mesoderm differentiation in the mouse embryo. Dev. Biol. 367, 1–14.

Partanen, J., Schwartz, L., Rossant, J., 1998. Opposite phenotypes of hypomorphic and Y766 phosphorylation site mutations reveal a function for Fgfr1 in anteroposterior patterning of mouse embryos. Genes Dev. 12, 2332–2344.

Perantoni, A.O., Timofeeva, O., Naillat, F., Richman, C., Pajni-Underwood, S., Wilson, C., Vainio, S., Dove, L.F., Lewandoski, M., 2005. Inactivation of FGF8 in early mesoderm reveals an essential role in kidney development. Development 132, 3859–3871.

Pourquie, O., 2001. Vertebrate somitogenesis. Annu. Rev. Cell Dev. Biol. 17, 311–350.

Sakai, Y., Meno, C., Fujii, H., Nishino, J., Shiratori, H., Saijoh, Y., Rossant, J., Hamada, H., 2001. The retinoic acid-inactivating enzyme CYP26 is essential for establishing an uneven distribution of retinoic acid along the anterio-posterior axis within the mouse embryo. Genes Dev. 15, 213–225.

Sawada, A., Shinya, M., Jiang, Y.J., Kawakami, A., Kuroiwa, A., Takeda, H., 2001. Fgf/MAPK signalling is a crucial positional cue in somite boundary formation. Development 128, 4873–4880.

Shum, A.S., Copp, A.J., 1996. Regional differences in morphogenesis of the neuroepithelium suggest multiple mechanisms of spinal neurulation in the mouse. Anat. Embryol. 194, 65–73. (Berl).

Shum, A.S., Poon, L.L., Tang, W.W., Koide, T., Chan, B.W., Leung, Y.C., Shiroishi, T., Copp, A.J., 1999. Retinoic acid induces down-regulation of Wnt-3a, apoptosis and diversion of tail bud cells to a neural fate in the mouse embryo. Mech. Dev. 84, 17–30.

Stadler, H.S., Higgins, K.M., Capecchi, M.R., 2001. Loss of Eph-receptor expression correlates with loss of cell adhesion and chondrogenic capacity in Hoxa13 mutant limbs. Development 128, 4177–4188.

Storm, E.E., Garel, S., Borello, U., Hebert, J.M., Martinez, S., McConnell, S.K., Martin, G.R., Rubenstein, J.L., 2006. Dose-dependent functions of Fgf8 in regulating telencephalic patterning centers. Development 133, 1831–1844.

Sun, X., Mariani, F.V., Martin, G.R., 2002. Functions of FGF signalling from the apical ectodermal ridge in limb development. Nature 418, 501–508.

Sun, X., Meyers, E.N., Lewandoski, M., Martin, G.R., 1999. Targeted disruption of Fgf8 causes failure of cell migration in the gastrulating mouse embryo. Genes Dev. 13, 1834–1846.

Takada, S., Stark, K.L., Shea, M.J., Vassileva, G., McMahon, J.A., McMahon, A.P., 1994. Wnt-3a regulates somite and tailbud formation in the mouse embryo. Genes Dev. 8, 174–189.

ten Berge, D., Brugmann, S.A., Helms, J.A., Nusse, R., 2008. Wnt and FGF signals interact to coordinate growth with cell fate specification during limb development. Development 135, 3247–3257.

Tzouanacou, E., Wegener, A., Wymeersch, F.J., Wilson, V., Nicolas, J.F., 2009. Redefining the progression of lineage segregations during mammalian embryogenesis by clonal analysis. Dev. Cell 17, 365–376.

Vermot, J., Gallego Llamas, J., Fraulob, V., Niederreither, K., Chambon, P., Dolle, P., 2005. Retinoic acid controls the bilateral symmetry of somite formation in the mouse embryo. Science 308, 563–566.

Wahl, M.B., Deng, C., Lewandoski, M., Pourquie, O., 2007. FGF signaling acts upstream of the NOTCH and WNT signaling pathways to control segmentation clock oscillations in mouse somitogenesis. Development 134, 4033–4041.

Wilson, V., Beddington, R.S., 1996. Cell fate and morphogenetic movement in the late mouse primitive streak. Mech. Dev. 55, 79–89.

Wilson, V., Olivera-Martinez, I., Storey, K.G., 2009. Stem cells, signals and vertebrate body axis extension. Development 136, 1591–1604.

Xu, X., Li, C., Takahashi, K., Slavkin, H.C., Shum, L., Deng, C.X., 1999. Murine fibroblast growth factor receptor 1alpha isoforms mediate node regression and are essential for posterior mesoderm development. Dev. Biol. 208, 293–306.

Yoshikawa, Y., Fujimori, T., McMahon, A.P., Takada, S., 1997. Evidence that absence of Wnt-3a signaling promotes neuralization instead of paraxial mesoderm development in the mouse. Dev. Biol. 183, 234–242.